Molecular Staging of Epithelial Maturation Using Secretory Cell–Specific Genes as Markers

Anna C. Zemke[1], Joshua C. Snyder[1,2], Brian L. Brockway[1,2], Jeffrey A. Drake[1,2], Susan D. Reynolds[1], Naftali Kaminski[3], and Barry R. Stripp[1,2]

[1]Center for Lung Regeneration, Department of Environmental and Occupational Health; [3]The Dorothy P. and Richard P. Simmons Center for Interstitial Lung Diseases, Pulmonary Allergy and Critical Care Medicine, University of Pittsburgh, Pittsburgh, Pennsylvania; and [2]Division of Pulmonary, Allergy and Critical Care Medicine, Duke University Medical Center, Durham, North Carolina

Bronchiolar Clara cells undergo phenotypic changes during development and in disease. These changes are poorly described due to a paucity of molecular markers. We used chemical and transgenic approaches to ablate Clara cells, allowing identification of their unique gene expression profile. Flavin monooxygenase 3 (*Fmo3*), paraoxonase 1 (*Pon1*), aldehyde oxidase 3 (*Aox3*), and claudin 10 (*Cldn10*) were identified as novel Clara cell markers. New and existing Clara cell marker genes were categorized into three classes based on their unique developmental expression pattern. *Cldn10* was uniformly expressed in the epithelium at Embryonic Day (E)14.5 and became restricted to secretory cells at E18.5. This transition was defined by induction of CCSP. Maturation of secretory cells was associated with progressive increases in the expression of *Fmo3, Pon1, Aox3,* and *Cyp2f2* between late embryonic and postnatal periods. Messenger RNA abundance of all categories of genes was dramatically decreased after naphthalene-induced airway injury, and displayed a sequence of temporal induction during repair that suggested sequential secretory cell maturation. We have defined a broader repertoire of Clara cell–specific genes that allows staging of epithelial maturation during development and repair.

Keywords: Clara; Claudin-10; bronchiole; differentiation; lung development

Mammalian conducting airways are lined by a heterogeneous population of nonciliated secretory cells, including goblet, serous, and Clara cells (1). Clara cells are classically defined as nonciliated, columnar cells with abundant endoplasmic reticulum and dense secretory granules (2). Clara cells fitting this definition are restricted to the bronchiolar epithelium, where they contribute from 50 to 80% of the cellularity in mice (1). More recently, Clara cells have been defined by expression of specific genes allowing for the application of molecular criteria to describe their phenotype. This molecular phenotype allows for quantitative measurement of epithelial phenotype both within the entire lung and on an individual cellular basis. Clara Cell Secretory Protein (CCSP or secretoglobin 1a1) is the most commonly used molecular marker; however, the use of CCSP as a molecular marker can lead to confusion, as CCSP is expressed by other secretory cell subsets of the mammalian airway (3, 4). There are currently very few molecular markers that distinguish epithelial subpopulations within the lung. Development of a wider array of such markers would facilitate studies of epithelial maturation and repair.

(*Received in original form October 22, 2007 and in final form August 19, 2008*)

This research was funded by RO1 HL064888 (to B.R.S.). These studies were also supported by NIH grants HL090146 and ES015960.

Correspondence and requests for reprints should be addressed to Barry R. Stripp, Department of Medicine, Division of Pulmonary, Allergy and Critical Care Medicine, 2075 MSRBII, 106 Research Drive, DUMC Box 103000, Durham, NC 27710. E-mail: Barry.Stripp@Duke.edu

Am J Respir Cell Mol Biol Vol 40. pp 340–348, 2009
Originally Published in Press as DOI: 10.1165/rcmb.2007-0380OC on August 28, 2008
Internet address: www.atsjournals.org

CLINICAL RELEVANCE

Few genes exist to define cell types of the airway and disease-related changes that accompany epithelial remodeling. We identify new genes that define distinct stages of secretory cell differentiation in the developing and repairing airway.

Airway lineages are specified during embryogenesis and undergo a process of differentiation that initiates in proximal airways. Ciliated cells of the developing mouse airway appear between Embryonic Day (E)14 and E16 (days post-coitum [dpc]), depending on the method of identification (5, 6). Currently, the earliest molecular marker of secretory cell differentiation is CCSP, which is expressed at very low levels beginning at E15.5 dpc and much higher levels immediately before birth (7–9). The airway epithelium is structurally and functionally immature at birth. Clara cells contain abundant glycogen at birth, which is lost within the first days of life (7, 10). The secretory apparatus acquires the adult ultrastructural appearance by 3 weeks of age, and adult xenobiotic metabolizing capacity is not reached until more than 4 weeks of age (7, 8). The expression of molecular markers also changes during postnatal development. By immunohistochemistry, adult levels of CCSP are found by 2 weeks, while members of the cytochrome P450 family require 4 weeks to reach adult expression levels (8). In addition to the normal process of developmental maturation seen within bronchiolar Clara cells, there is evidence of functionally immature populations of nonciliated cells that are maintained within the adult airway. A rare subset of CCSP-expressing cells can be distinguished from Clara cells on the basis of their resistance to the cytochrome P450-bioactivated toxicant naphthalene (11).

There are limited molecular markers available to distinguish developmental, spatial, or functional subsets of secretory cells. The expression of two secretoglobin family members distinguish very proximal (*Scgb3a1*) from more distal (*Scgb3a2*) secretory cells in the mouse (12). Acidic mammalian chitinase and Ym1 chitinase distinguish secretory populations based upon their propensity to undergo mucus cell metaplasia (13). However, these existing molecular markers only allow for a crude characterization of postnatal airway maturation. In addition to steady-state heterogeneity, chronic lung diseases such as asthma, bronchopulmonary dysplasia, and chronic bronchitis cause phenotypic changes within the secretory cell population. These changes include loss of Clara cells, decreased CCSP expression, and increased production of mucus (14–16). Given the progenitor role that has been ascribed to Clara cells, the existence of multiple secretory cell subpopulations, and the phenotypic changes seen in human disease states, we sought to further characterize the molecular phenotype of airway secretory cells by expanding the available repertoire of molecular markers that can be used to follow their postnatal maturation. Using mouse models allowing

conditional ablation of either naphthalene-sensitive secretory cells or total CCSP-expressing cells, we have defined novel marker genes whose developmental expression pattern at the mRNA level and subcellular distribution at the protein level defines different stages of secretory cell maturation.

MATERIALS AND METHODS

Animal Husbandry

Colonies of wild-type FVB/n mice and CCSP-HSVtk mice on an FVB/n background were maintained as an in-house breeding colony under specific pathogen–free conditions in an AAALAC-accredited facility. All procedures involving animals were approved by the Institutional Animal Care and Use Committee of the University of Pittsburgh.

Genotyping

CCSP-HSVtk mice were genotyped by polymerase chain reaction (PCR) for the presence of a herpes virus thymidine kinase amplicon as previously described (17).

Naphthalene Administration

Adult (8- to 10-wk-old) male mice FVB/n mice were used for all naphthalene exposures. Naphthalene (Sigma, St. Louis, MO) was dissolved in Mazola corn oil and injected intraperitoneally at a dose of 275 mg/kg. All injections were performed between 8:00 and 10:00 A.M. to normalize injury responses (11). Untreated animals were used as controls.

Ganciclovir Administration

Ganciclovir was administered as previously described (18). CCSP-HSVtk transgenic mice were exposed to ganciclovir (4.5 mg/d), which was administered using 14-day mini-osmotic pumps (ALZET Osmotic Pumps, #2001D; ALZA Corp., Palo Alto, CA). Cytovene-IV (GCV sodium; Hoffmann-La Roche, Inc., Nutley, NJ) was dissolved in sterile normal saline to give a final concentration of 375 mg/ml. Untreated animals were used as controls.

Tissue Recovery for RNA Isolation and Histology

Mice were anesthetized using Avertin, exsanguinated, and the trachea cannulated. Mice were lavaged extensively with sterile saline, and lung lobes homogenized. RNA was prepared from whole lung homogenate as described by Chomczynski and Sacchi (19). For histology, lungs were inflation-fixed *in situ* with 10% formalin for 10 minutes and immersion-fixed for a minimum of 2 hours. Tissue was cryoprotected and degassed overnight before being frozen in Tissue-Tek OCT (Pittsburgh, PA). Embryonic tissue was immersion fixed with 10% formalin and cryoprotected as above.

Microarray Analysis

Total mouse lung RNA was isolated as described above. Four biological replicates were used for all time points. Unexposed mice were used as controls for both experiments. RNA samples were purified using RNAeasy kits according to the manufacturer's instructions (Qiagen, Germantown, MD). Affymetrix Cat# 900493 GeneChip Expression 3'Amplification One-Cycle Target Labeling and Control Reagent kit was used to produce cRNA (Affymetrix, Santa Clara, CA). CodeLink UniSet Mouse 20K I Bioarrays (GE Healthcare Bio-Sciences Corp., Piscataway, NJ) were used for gene expression analysis. Determination of RNA quality, generation of biotin-labeled cRNA, hybridization to the Bioarray, scanning, and data collection were conducted through the University of Pittsburgh Cancer Institute Clinical Genomics Facility according to the manufacturer's protocol.

Bioinformatics

Genes that did not pass the manufacturer's recommendation for signal quality were excluded from further analysis. After filtering, 18,048 genes were present. Complete data tables were compiled including full annotations using the freeware program Source (Stanford University, Stanford, CA) and Microsoft Access (Redmond, WA). Subsequent data analysis was performed as described previously (20–22). Data were normalized and statistical analysis performed to determine significant changes in gene expression within each model. Data were imported into ScoreGenes Software Package (Jerusalem, Israel) for data normalization and statistical analyses. Significant gene expression changes were defined as fulfilling a Student's t test P value < 0.05 and a threshold number of misclassifications (TNOM) of $\leqslant 1$. Next, genes defined as significant by both criteria at 2 days after naphthalene exposure and either 6 or 9 days after ganciclovir exposure were identified.

RNA Abundance

Quantitative RT-PCR (Q-PCR) was used to assess mRNA abundance. cDNA was prepared and assayed as previously described (23). Differential gene expression was determined using an ABI PRISM 7000 Sequence Detection System and values calculated by the method described by Heid and coworkers using a standard total lung RNA preparation as calibrator (24). Equal amounts of mRNA were used for each cDNA synthesis reaction. All RT-PCR reactions were done in duplicate for each sample. Good agreement was seen between duplicates. Assays-on-Demand gene expression probes were purchased from Applied Biosystems, Foster City, CA. The following probes were used: Mm00457974_m1 (*Cldn10*), Mm00514964_m1 (*Fmo3*), Mm00508163_m1 (*Aox3*), Mm00446953_m1 (*Gusb*), Mm01158777_m1 (*Pon1*), Mm00484087_m1 (*Cyp2f2*), Mm00488144_m1 (*Sftpc*), and Mm00442026_m1 (*CCSP*).

Immunofluorescence

Immunofluorescence techniques were used to detect Cldn10 (rabbit, cat#388400, 1:1,000, or mouse monoclonal IgG1, cat#415100; Invitrogen, Carlsbad, CA), β-catenin (mouse IgG_1, cat #610154, 1:500; BD Transduction Labs, San Jose, CA), CCSP (rabbit or goat, in house, 1:20,000) and ZO-1 (rabbit, cat#40-2200, 1:100; Zymed). Frozen sections were post-fixed in 10% neutral buffered formalin for 10 minutes, rinsed in distilled water, and blocked with 5% BSA/PBS. Primary antibodies were diluted in BSA/PBS, applied to slides and incubated for 2 hours at room temperature, washed, and secondary antibodies were applied to slides for 2 hours at room temperature. All secondary antibodies were purchased from Molecular Probes (Invitrogen). Coverslips were mounted using Fluoromount-G (Southern Biotech, Birmingham, AL) containing 2 μg/ml 4,6,diamidino-2-phenylindole (DAPI; Sigma). Antigen–antibody complexes were visualized as single optical planes using an Olympus Fluoview confocal microscope (Center Valley, PA) equipped with Nomarski optics for simultaneous brightfield detection (optical sections of 45 μm). Images were acquired using ImagePro (Silver Spring, MD) and processed using Metamorph software packages (Sunnyvale, CA).

Statistics

ANOVA analysis was performed using Minitab software (State College, PA). A P value of $\leqslant 0.05$ was considered significant. Determination of statistical significance of real-time PCR data involving a time course and two genotypes was done using a general linear model (two-way ANOVA type). Genotype and time were used as factors, with mRNA abundance as a response factor. In the case of statistical significance, a *post hoc* Tukey test was used.

RESULTS

Models of Clara Cell Depletion

Two models of airway injury were used in this study: naphthalene-induced Clara cell ablation and ganciclovir-mediated ablation of CCSP-expressing cells in CCSP-HSVtk transgenic mice. These models differed in the spectrum of target cells injured and the ensuing repair response. Naphthalene-mediated Clara cell ablation is repaired through activation of naphthalene-resistant CCSP-expressing stem cells (11). In contrast, ganciclovir-mediated ablation of CCSP-expressing cells in CCSP-HSVtk transgenic mice is not accompanied by a productive repair process because the CCSP-expressing stem cells required for repair are also ablated (17).

Two days after naphthalene exposure, abundance of the Clara cell–specific mRNA *CCSP* decreased to 7.3% ± 2.6, and

Cyp2f2 decreased to 6.9% ± 2.6 of control levels within total lung RNA ($P < 0.05$ for both genes, Figure 1A). The abundance *Cyp2f2* began to increase by Day 6, reflecting the previously described repair process (11). During this period there was no decrease in *Sftpc* mRNA abundance (Figure 1A). Exposure of CCSP-HSVtk mice to GCV for 3 days resulted in the development of airway injury that was accompanied by reductions in the abundance of *CCSP* and *Cyp2f2* mRNAs within total lung RNA. By the ninth day of continuous GCV exposure, levels of *CCSP* and *Cyp2f2* mRNAs had decreased to 6.4% ± 3.5 and 5.8% ± 3.1 of their control levels, respectively ($P < 0.05$ for both genes, Figure 1B). Beginning at Day 6, a drop in *Sftpc* mRNA was observed reflecting the inflammatory response and collateral alveolar changes previously described in this model (25). However, this drop did not reach statistical significance by one-way ANOVA (Figure 1B). These data confirmed that the lung tissue used for further microarray analysis showed the previously described pattern of injury and repair.

Identification of Putative Clara Cell Markers

Codelink mouse 20K microarrays were used to identify genes that significantly decreased after Clara cell depletion. At 2 days after naphthalene administration, 742 genes decreased by more than 2-fold when compared with the corresponding control group. In the CCSP-HSVtk model, 35 genes decreased at Day 6, and 65 genes decreased by Day 9 when compared with control. As show in Table 1, 19 genes were identified that decreased in both models of Clara cell depletion. Genes were selected for further analysis if they decreased more than 2-fold, had $P <$ 0.05, a threshold number of misclassifications (TNOM) of 0 at 2 days after naphthalene treatment, and met the same criteria at either Day 6 or Day 9 of ganciclovir exposure in the CCSP-HSVtk model. Of these genes, *Cyp2f2* (NM_007817), *CCSP* (NM_11681), and Secretoglobin 3A2 (NM_054038) are well-described Clara cell genes (12, 26). We selected the following genes that met these criteria for further analysis: paraoxonase 1 (*Pon1*), flavin containing monooxygenase 3 (*Fmo3*), aldehyde oxidase 3 (*Aox3*), and claudin 10 (*Cldn10*).

Application of Novel Secretory Cell Markers to Follow Developmental Maturation of the Airway Epithelium

Existing and newly identified markers for secretory cell maturation were applied to the analysis of epithelial cell differentiation that accompanied late embryonic and postnatal lung development. Developmental expression of putative secretory cell markers was determined in total lung mRNA from E17.5 dpc through adulthood. Genes could be classified into two general categories based upon their developmental expression patterns. *Aox3* and *Pon1* showed a large increase in mRNA abundance between Day 14 and adulthood (Figure 2B) that mirrored the increase in mRNA abundance seen in *Cyp2f2*. Expression of these three genes (*Aox3*, *Pon1*, and *Cyp2f2*) approximately tripled between birth and adulthood. This increase was statistically significant for all three genes. *Fmo3* was undetectable before Day 28, when it was expressed at 28% of adult levels. *Cldn10* showed a different developmental expression pattern. At E17.5 dpc, mRNA abundance was 129.9 ± 9.4% that of adult control mice. By Postnatal Day 3, *Cldn10* mRNA abundance dropped to only 39.3% ± 9.7 of adult mRNA abundance, after which it gradually rose to adult abundance (Figure 2A).

Novel Secretory Markers to Follow Epithelial Differentiation in Repairing Airways

We used existing and newly identified secretory markers to follow epithelial differentiation during recovery from naphthalene exposure. Quantitative real-time PCR was used to determine mRNA abundance. As shown in Figure 3, *Pon1*, *Fmo3*, and *Cldn10* mRNAs all showed statistically significant reductions of greater than 90% after naphthalene treatment ($P <$ 0.05 by Tukey test for all three genes). Aox3 was the only exception, which, under the conditions of naphthalene treatment used (250 mg/kg naphthalene), showed a dramatic early increase in mRNA abundance within the first 12 hours of exposure (data not shown), with a subsequent decrease to 15% of peak levels by the 2-day recovery time point that represented 46% of steady-state levels (Figure 3B). In the following recovery period, *Cldn10* recovered the most rapidly (53.6 ± 10% of control at Day 5). *Fmo3* and *Pon1* both showed

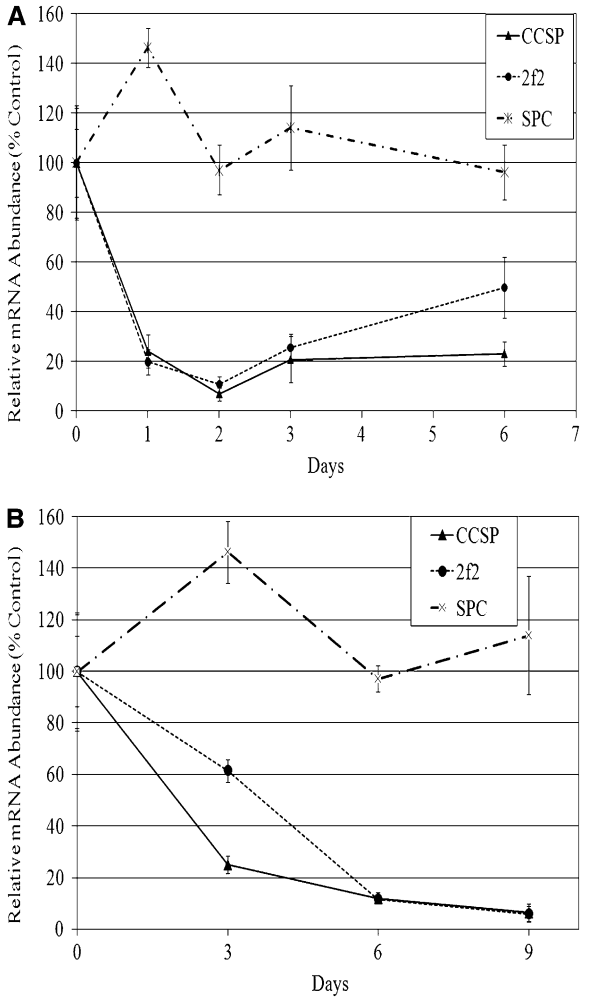

Figure 1. Clara cell depletion in naphthalene and HSVtk models. (*A*) Wild-type or (*B*) CCSP-HSVtk transgenic mice were exposed to naphthalene (275 mg/kg) or ganciclovir, respectively, and expression of *CCSP*, *Cyp2f2*, and *Sftpc* was assayed by quantitative real-time PCR in total lung RNA ($n = 4$). All RT-PCR data are shown normalized to % mean mRNA abundance within unexposed control mice, with *error bars* indicating SEM. (*A*) Naphthalene exposure caused a 90% reduction in both *CCSP* and *Cyp2f2* mRNA abundance by Day 2 ($P < 0.05$ for both *CCSP* and *Cyp2f2*, control versus later time points by one-way ANOVA). No statistically significant change was seen in *Sftpc* mRNA abundance. (*B*) Ganciclovir-mediated Clara cell ablation decreased *CCSP* and *Cyp2f2* mRNA abundance to less than 10% of untreated control by Recovery Day 9 ($P < 0.05$ for both *CCSP* and *Cyp2f2*, control versus later time points by one-way ANOVA). No statistically significant decrease in Sftpc mRNA abundance was seen with ganciclovir exposure.

TABLE 1. PUTATIVE CLARA CELL TRANSCRIPTS

		Naphthalene Day 2		CCSP-HSV tK Day 6		CCSP-HSV tK Day 9	
Gene	Description	TNOM	Fold Change	TNOM	Fold Change	TNOM	Fold Change
NM_172484	RIKEN cDNA E030049G20 gene	0	−2.0	0	−1.9	0	−2.4
NM_007902	Endothelin 2	0	−2.1	0	−2.3	0	−2.4
AK01708		0	−2.2	1	−2.2	0	−2.4
NM_007817	Cytochrome P450, family 2, subfamily f, polypeptide 2	0	−2.3	0	−1.9	0	−4.1
NM_021386	Claudin 10 (Cldn10), transcript	0	−2.5	0	−2.0	0	−3.5
NM_008286	Strain B10.S/DvTe histamine receptor H2 (Hrh2)	0	−2.7	0	−2.5	0	−3.0
BG795288	Transcribed locus	0	−2.7	0	−2.7	0	−2.7
NM_009381	Thyroid hormone responsive SPOT14 homolog	0	−3.1	0	−2.8	0	−3.1
NM_011681	Secretoglobin, family 1A, member 1 (uteroglobin)	0	−3.1	0	−1.7	0	−3.7
AF306532	Chemokine (C-C motif) receptor-like 1 (C cr11)	0	−3.2	0	−3.1	0	−5.4
BC031432	CDNA clone MGC:6757	0	−3.6	0	−3.0	0	−2.9
NM_021456	Carboxylesterase 1	0	−4.8	0	−2.7	0	−2.4
NM_146017	Gamma-aminobutyric acid (GABA-A) receptor, pi	0	−4.8	0	−3.3	0	−7.2
NM_023617	Aldehyde oxidase 3 (*Aox3*)	0	−5.2	0	−3.1	0	−3.0
AW909485	PREDICTED: leucine-rich repeats and calponin homtrun -1ology (CH) domain containing 1	0	−5.4	1	−2.8	0	−2.2
NM_008030	Flavin containing monooxygenase 3 (Fmo3)	0	−6.0	0	−3.1	1	−2.2
NM_144930	Expressed sequence AU018778	0	−7.8	0	−3.3	0	−2.8
NM_054038	Secretoglobin, family 3A, member 2 (Scgb3a2)	0	−8.5	0	−3.9	0	−19.1
NM_011134	Paraoxonase 1	0	−12.1	0	−6.1	0	−15.9

Definition of abbreviations: TNOM, Threshold number of misclassifications.

delayed recovery kinetics (24.1 ± 8.5% and 34.1 ± 12.6% at Day 5, respectively) that were similar to that of *CCSP* (21.6 ± 4.2% at Day 5). Recovery of mice for 30 days resulted in restoration of *CCSP* and *Cyp2f2* mRNAs to near steady-state levels (108 ± 29% and 72 ± 8%, respectively). In contrast, a subset of genes defined by Aox3, Pon1, and FoxJ1 were expressed at elevated levels (163 ± 16%, 230 ± 105%, and 223 ± 71%, respectively) relative to the steady-state condition at the late recovery time point, indicating that renewal of the injured epithelium results in subtle changes in the molecular phenotype of both secretory and ciliated cells. In the CCSP-HSVtK model, *Pon1*, *Fmo3*, *Aox3*, and *Cldn10* decreased to less than 30% of control at Day 6 after ganciclovir administration. After 9 days of continuous ganciclovir exposure, the expression of the putative Clara cell markers was as follows: *Pon1*, 1.2% ± 0.3; *Fmo3*, 8.9% ± 3.3; *Aox3*, 11.6% ± 4.4; *Cldn10*, 13.2% ± 5.1. This expression pattern after airway injury is consistent with the identified genes being expressed within the Clara cell population, but suggests that renewal after naphthalene injury results in adaptive changes to both secretory and ciliated cells.

Subcellular Localization of Claudin 10

Because *Cldn10* shows a Clara cell–specific expression pattern in the naphthalene and ganciclovir models, but shows a distinct pattern of developmental regulation to those of phase I metabolizing enzymes, we determined the cellular and subcellular distribution of Cldn10 using confocal immunofluorescence microscopy. Cldn10 (*red*) co-localized with β-catenin (*green*) along the lateral membrane of conducting airway epithelial cells (Figure 4A; compare the subcellular distribution of Cldn10 in *red* with β-catenin in *green*). It was not limited to the spatial domain of ZO-1 immunoreactivity (Figure 4B). Punctate ZO-1 staining is seen at the apical edge of the lateral membrane, while β-catenin staining is seen along the entire basolateral membrane. In addition, a cytoplasmic pool of Cld10 was seen in cells showing strong lateral membrane staining.

Cellular and Developmental Expression Pattern of Claudin 10

To determine the cellular localization of Cldn10, we colocalized Cldn10 immunoreactivity with the Clara cell marker CCSP by confocal immunofluorescence microscopy. Cldn10 was specifically localized to the lateral plasma membrane of CCSP-immunoreactive cells (Figures 4C–4F). Cell junctions between adjacent cells that were negative for CCSP immunoreactivity lacked Cldn10 staining (*arrowheads* in Figure 4C and *arrows* in Figure 4F). No lateral membrane Cldn10 staining was observed between adjacent FoxJ1-immunoreactive cells (Figures 4G–4I) or CGRP-immunoreactive cells (Figures 4J–4L), indicating a lack of Cldn10 expression within ciliated and neuroendocrine cells, respectively. No staining was seen in the alveolar space, vasculature, or mesenchyme. In addition, no differences in Cldn10 distribution were seen along the proximal-distal axis of the intrapulmonary airway (not shown).

Cldn10 mRNA and protein expression was detected in developing airways. At E14.5 dpc, low levels of Cldn10 immunoreactivity were observed throughout the developing airway epithelium (Figure 5A). At this developmental stage, Cldn10 immunofluorescence was uniformly distributed among all epithelial cells. In addition to lateral membrane localization, a significant cytoplasmic pool was seen. By E18.5, expression of Cldn10 was restricted to CCSP-expressing cells (Figure 5C). However, at this time point, expression levels per cell were similar to those of the adult, the cytoplasmic pool had decreased, and Cldn10 was concentrated at the lateral plasma membrane (Figures 5B and 5C). By the fifth postnatal day, Cldn10 immunoreactivity remained restricted to the CCSP-immunoreactive subset of airway epithelial cells (Figure 5D). These cells exhibited high CCSP immunofluorescence compared with earlier developmental time points.

We next sought to determine the distribution of Cldn10 after naphthalene exposure. At Day 2 after naphthalene, rare Cld10- and CCSP-immunoreactive cells could be seen in proximity to clusters of CGRP-immunoreactive cells and in terminal bronchioles (Figures 6D–6F, and data not shown). Epithelial renewal was accomplished by expansion of CCSP/Cldn10-immunoreactive cells at each of these locations (Figures 6G–6O, and data not shown). Even though repair of the airway epithelium was largely complete by the 30-day recovery time point, clusters of ciliated cells that were devoid of adjacent CCSP/Cldn10-immunoreactive cells remained (Figures 6M–6O, and data not shown). These data support the conclusions that Cldn10 is a Clara cell–specific pro-

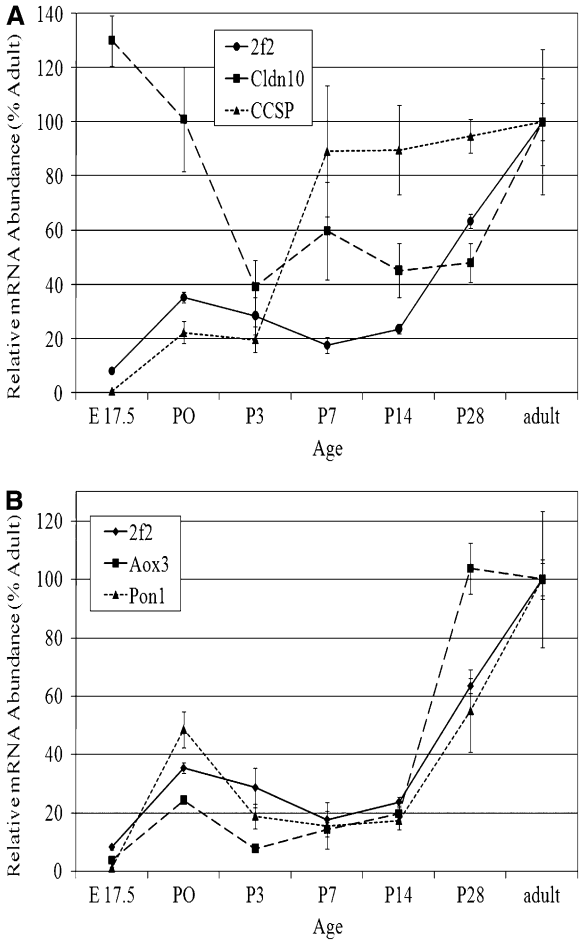

Figure 2. Expression of putative Clara cell markers during development. Expression of *Aox3*, *Cyp2f2*, *Pon1*, *CCSP* and *Cldn10* was assayed by RT-PCR in total lung mRNA from mice of different ages. Between three and six mice were used per time point (E17.5 refers to Embryonic Day 17.5; "P" refers to Postnatal Day of tissue collection). Expression was normalized to adult expression levels and presented as % adult mouse relative mRNA abundance with SEM. (*A*) *CCSP* and *Cldn10* show different developmental kinetics. *CCSP* increases between P3 and P7 (statistically significant by one-way ANOVA followed by Tukey analysis). *Cldn10* showed a second developmental pattern, dropping between E17.5 and P3 (the only significant time points by one-way ANOVA). (*B*) *Cyp2f2*, *Aox3*, and *Pon1* behave similarly. Significant increases in expression of all three mRNA species were observed across the time course (one-way ANOVA followed by Tukey analysis). *Aox3* mRNA abundance increases more rapidly than *Cyp2f2* or *Pon1* (statistically significant difference at P28 by general linear model followed by Tukey analysis). The difference in kinetics between *Cyp2f2* and *CCSP* is statistically significant at P7 and P14 (general linear model followed by Tukey analysis).

tein in the adult lung and that its expression defines nascent epithelium of the repairing airway.

DISCUSSION

We have used a combination of cell ablation strategies and microarray screening to identify the novel mRNA repertoire expressed by mature secretory cells of the conducting airway. These genes can be grouped into three categories by order of developmental maturation and recovery after naphthalene treatment. The first category was largely composed of known phase I metabolizing genes, including *Pon1*, *Aox3*, and *Fmo3*, which were regulated in a coordinate fashion with the known

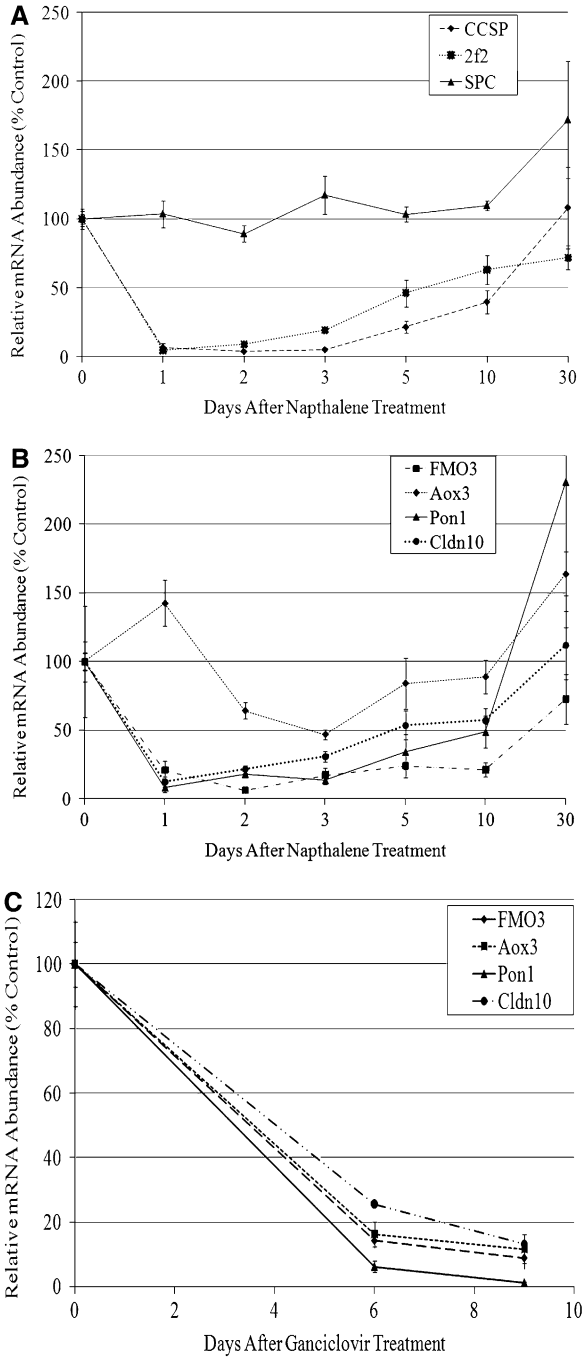

Figure 3. Expression of putative Clara cell markers after injury. Analysis of gene expression within the repairing lung of mice after naphthalene (250 mg/kg) or ganciclovir exposure. (*A*) Quantitative RT-PCR analysis of CCSP and Cyp2f2 mRNA abundance and SP-C mRNA abundance as measures of airway Clara and alveolar type 2 cells during repair after naphthalene-induced airway injury. (*B*) Quantitative RT-PCR analysis of Aox3, Fmo3, Pon1, and Cldn10 mRNA abundance during repair after naphthalene-induced airway injury. (*C*) Quantitative RT-PCR analysis of Aox3, Fmo3, Pon1, and Cldn10 mRNA abundance after ganciclovir-mediated ablation of CCSP-expressing cells in airways of CCSP-HSVtk transgenic mice. Four mice per time point were used in both experiments. *Error bars* show SEM.

Clara cell–specific xenobiotic metabolizing enzyme *Cyp2f2*. These genes were all late markers of Clara cell maturation in either developing or repairing airways. During lung development, mRNAs encoding these genes did not reach adult

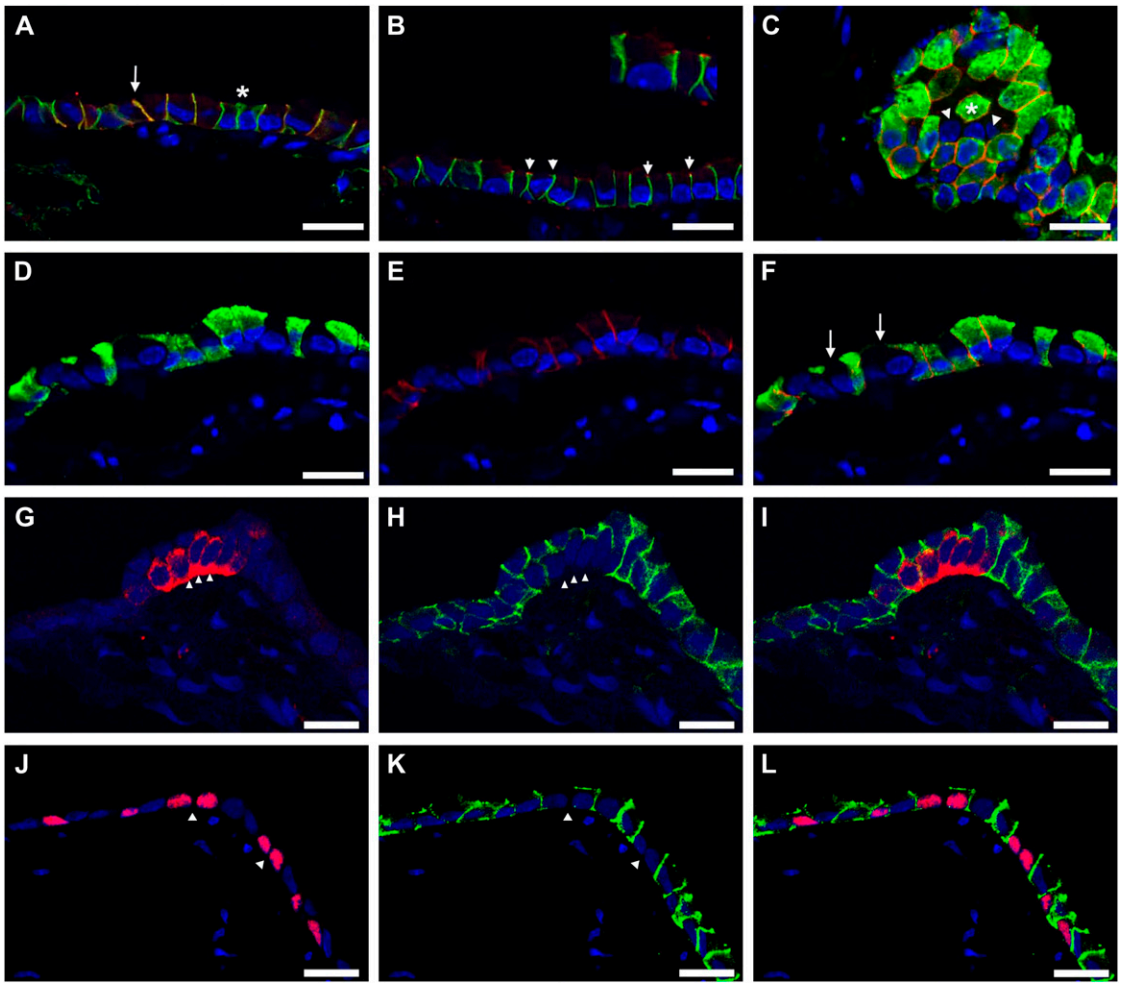

Figure 4. Subcellular and cell type–specific localization of Claudin 10. Immunolocalization of *Cldn10* was determined on frozen mouse lung sections with fluorescence detection and images acquired by confocal microscopy. (*A*) *Cldn10* staining (*red*) and β-catenin (*green*). *Arrow* shows a cell junction with both *Cldn10* and β-catenin staining along a lateral membrane. *Asterisk* shows a *Cldn10*-negative, β-catenin–positive cell junction. (*B*) β-*catenin* (*green*) and ZO-1 (*red*). The tight junction marker ZO-1 is seen as punctate staining at the apical tip of lateral membranes. β-catenin defines the adherens junction at the lateral membrane. *Inset* shows higher magnification regions with punctuate ZO-1 staining. (*C*) CCSP (*green*) and *Cldn10* (*red*). *Arrowheads* show CCSP-negative, *Cldn10*-negative cells. The *asterisk* indicates a CCSP-positive cell surrounded by a ring of CCSP-negative cells. *Cldn10* staining (*red*) is only seen around the center cell. (*D–F*) CCSP-immunoreactive cells (*green* in *D*) show lateral membrane staining for *Cldn10* (*red* in *E*). A small pool of cytoplasmic staining is also seen. (*F*) Merged image of *D* and *E* demonstrating that cell borders between CCSP-negative cells (*arrows*) lack *Cldn10* staining. Nuclear counter stain (DAPI) is seen in *blue*. (*G–I*) CGRP-immunoreactive cells (*red* in *G*) lack lateral membrane staining for *Cldn10* (*green* in *H*). *Arrowheads* identify junctions between CGRP-immunoreactive cells that are negative for *Cldn10*. (*I*) Merged image of *G* and *H*. Nuclear counterstain (DAPI) is seen in *blue*. (*J–L*) *FoxJ1*-immunoreactive cells (*red nuclei* in *J*) lack lateral membrane staining for *Cldn10* (*green* in *K*). *Arrowheads* identify junctions between *FoxJ1*-immunoreactive cells that are negative for *Cldn10*. (*L*) Merged image of *J* and *K*. Nuclear counterstain (DAPI) is seen in *blue*. All *scale bars* = 25 μm.

levels until Postnatal Days 28 (*Aox3*) to 60 (*Pon1* and *Cyp2f2*). Paraoxonase 1 (Pon1) is an esterase capable of hydrolyzing organophosphate compounds. Previously, it has been localized to nonciliated airway cells in the rat by immunohistochemistry (27). Flavin monooxygenases oxidize a wide variety of drugs and xenobiotic chemicals. Fmo3 has previously been localized to the mouse terminal bronchiole by *in situ* hybridization (28). Aldehyde oxidase 3 (also known as Aoh1) is a molybdoflavoprotein previously detected in mouse lung by Western blot (29). In addition to genes encoding xenobiotic metabolizing enzymes, carboxylesterase 1 (NM_021456) and an unidentified probe with greater than 90% homology with carboxylesterases (NM_144930) were decreased in both Clara cell ablation models and behaved as late markers of Clara cell maturation. The second category of genes that marked an intermediate stage of Clara cell maturation was composed of secreted proteins that included *CCSP* and the related secretoglobin *Scgb3a2*. These genes reached adult expression levels within the first 7 to 14 postnatal days, in agreement with previously published work (8). The third category was represented by *Cldn10*, which was identified as an early airway marker whose expression is subsequently restricted to Clara cells during developmental maturation of the epithelium.

The temporal sequence of marker gene expression observed during developmental maturation of airways was similar, albeit with significantly shortened kinetics, in the repairing epithelium after naphthalene exposure. Cldn10 and Aox3 expression were re-established more rapidly after injury. While Cldn10 was an early marker of airway differentiation in both developing and repairing airways, CCSP expression matured comparatively late during repair. Among the xenobiotic metabolizing enzymes studied, Aox3 matured most rapidly during development. Aox3 also differed from all other marker genes in the magnitude and kinetics of its altered expression during injury and repair. These results suggest that the repairing epithelium undergoes stages of repair that include epithelial renewal and maturation. Immaturity of airway secretory cells after injury and during the early phase of repair may contribute to altered epithelial function seen in chronic lung disease and the observation of tolerance to naphthalene-induced airway injury seen with repeated exposure (30).

We have identified Cldn10 as a valuable new marker to define immature airway epithelial cells whose expression is restricted to nonciliated cells of the mature epithelium. Claudins are classically thought to be tight junction proteins that contribute to regulation of paracellular trafficking of electrolytes and macromole-

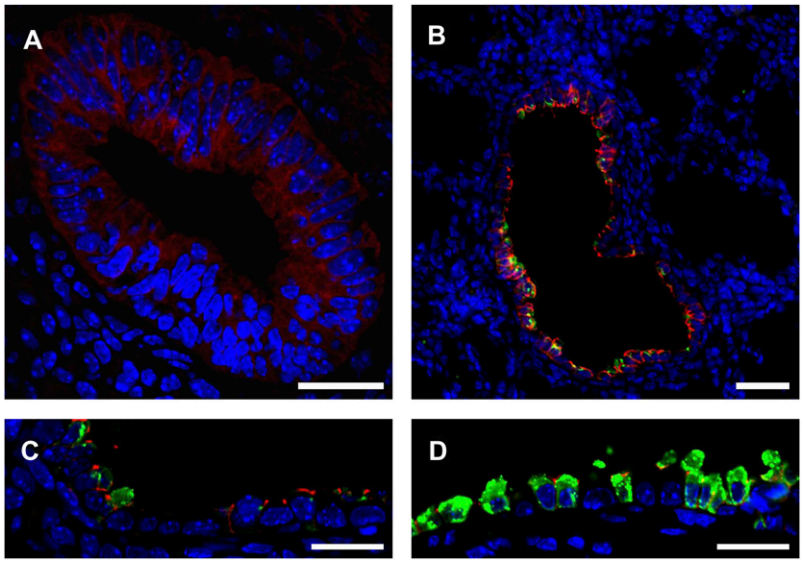

Figure 5. Claudin 10 is expressed early in mouse lung development. Mouse lungs from E14.55 or E18.5 embryos, or from P5 mice, were immunostained for localization of CCSP, *Cldn10*, and CGRP and images acquired by fluorescence microscopy. Nuclei were visualized using a DAPI nuclear counterstain (*blue*). (*A*) *Cldn10* (*red*) is expressed throughout the developing airway tubules at E14.5. *Scale bar* = 25 μm. (*B*) Intense *Cldn10* staining (*red*) is seen along lateral membranes of airway epithelial cells. Faint CCSP immunostaining (*green*) is seen within the airway at this developmental stage. *Scale bar* = 120 μm. (*C*) Tissue from E18.5 dpc embryos was stained as above. A row of four CCSP-negative, *Cldn10*-negative cells is seen surrounded by epithelial cell with strong *Cldn10* lateral membrane staining and weak CCSP staining. *Scale bar* = 25 μm. (*D*) Lung tissue from a 5-day-old mouse was immunostained as above. CCSP expression has greatly increased, and *Cldn10* staining remains restricted to CCSP immunoreactive cells. *Scale bar* = 25 μm.

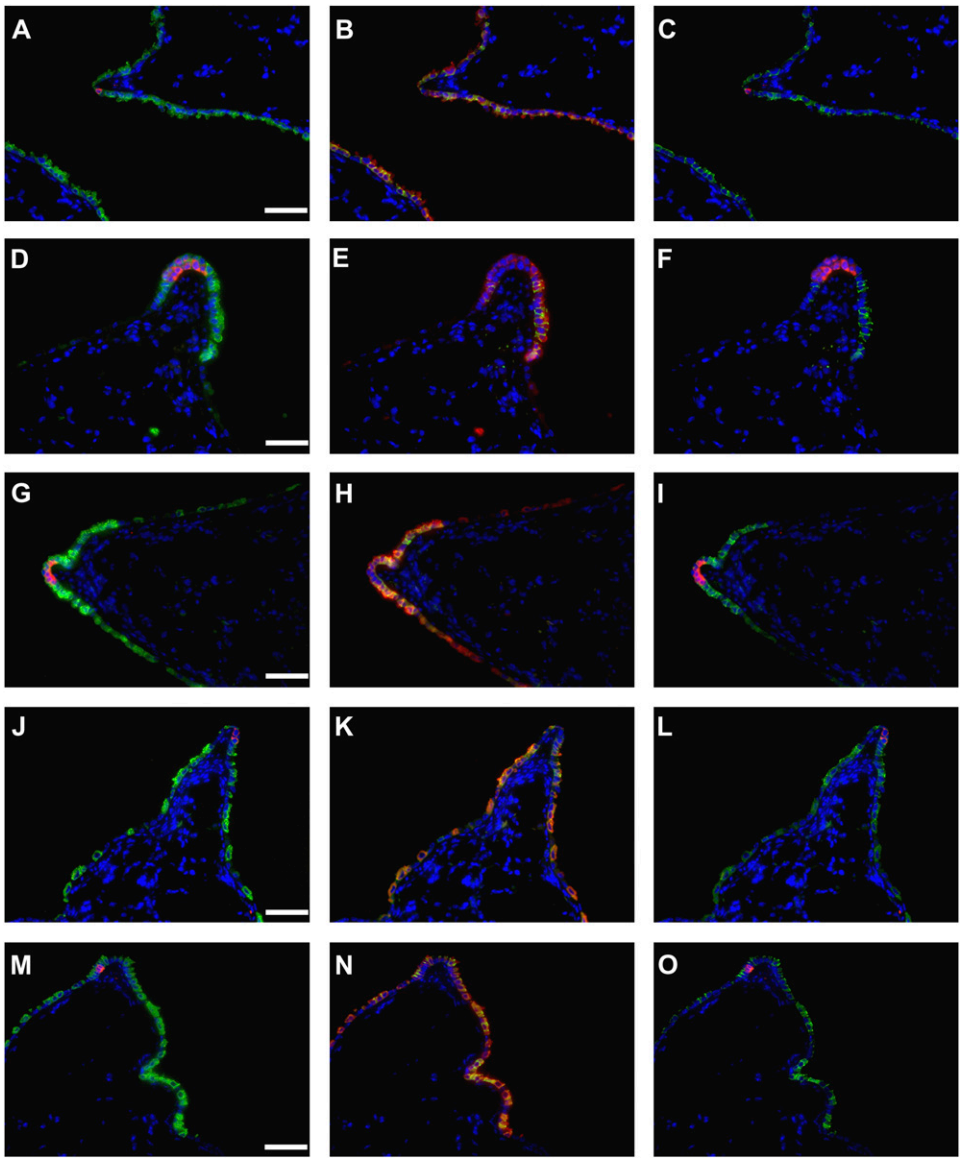

Figure 6. Expression of *Cldn10* during repair of naphthalene-injured airways. Frozen lung tissue sections were prepared from either control mice (*A–C*) or naphthalene-exposed mice that were recovered for either 2 days (*D–F*), 5 days (*G–I*), 10 days (*J–L*), or 30 days (*M–O*). Sections were immunostained for colocalization of either CCSP and CGRP (*green* and *red*, respectively, in *panels on left*), *Cldn10* and CCSP (*green* and *red*, respectively, in *center panels*), and *Cldn10* and CGRP (*green* and *red*, respectively, *panels on right*), and images acquired by conventional fluorescence microscopy. *Scale bars* = 50 μm.

cules. Interestingly, of the two splice variants of Cldn10 that are known to exist, Cldn10b is expressed in the lung. This splice variant has been shown to confer cation selectivity to paracellular transport in the kidney (31). However, Cldn10 was immunolocalized along the entire lateral surface of CCSP-expressing cells in both proximal and distal mouse airways. It was not found at the lateral membranes of either ciliated cells or pulmonary neuroendocrine cells within bronchioles. This cellular localization is in contrast with a previous report using the same antibody for immunolocalization of Cldn10 in mouse airway, which reported selective tight junction localization (31). However, the previously published data do not exclude lateral membrane localization of Cldn10 because of the *en face* airway sections used for analysis.

There is ample precedent for claudin localization outside of the tight junction. Within the airway, claudins-3 and -5 were found exclusively at the tight junction. However, claudins-1 and -4 were found along the entire lateral membrane, while claudin-7 was located along the lateral membrane and excluded from the tight junction (32). Cldn10 has been localized along the entire lateral membrane of exocrine glands and scattered epithelial cells of the cecum (31, 33). Our work colocalizes Cldn10 with β-catenin, an adherens junction protein. While the physiologic function of claudins found in the adherens junctions is unknown, it is possible that claudins are also involved in cell–cell adhesion or signaling, in addition to regulating paracellular permeability.

Clara cells are known to express xenobiotic metabolizing enzymes (notably cytochrome p450 family members) and a variety of immunomodulatory proteins of the secretoglobin and surfactant families. Genes encoding previously identified secretory products of airway epithleial cells, including secreteoglobins 3A1, 1A1, and 3A2 and PLUNC, were all significantly decreased within airways of ganciclovir-exposed CCSP-HSVtk transgenic mice (12, 34). Other significantly downregulated genes included numerous members of the Cyp450 family, including 2f2, 2a4, and 1a1 isoforms. The presence of previously known secreteoglobins and Cyp450 family members validated our approach of interrogating gene expression within total lung RNA for the identification of Clara cell–specific changes in gene expression. Because our computation approach required that putative Clara cell markers were decreased in both injury models, genes that differentiate the repair response between these models would not be detected. A potentially important category of cells whose abundance will differ between these experimental models of airway injury would be the naphthalene-resistant bronchiolar stem cells previously described by us and others (35–37). A technical limitation for our data set that precluded this analysis was the finding that comparatively few genes were identified within the CCSP-HSVtk model compared to the naphthalene model despite the greater severity of injury and inflammation in gancyclovir-exposed CCSP-HSVtK mice. This result likely reflected greater variability within the CCSP-HSVtk data set. Our finding of novel marker genes to follow secretory cell maturation in the developing and repairing lung will provide valuable tools to better define aberrations in these processes associated with lung tissue remodeling. Further refinement of these approaches may allow identification of genes whose expression is restricted to the bronchiolar stem cell.

Conflict of Interest Statement: N.K. is a recipient of an investigator-initiated grant of $674,800 from Biogen Idec on pulmonary fibrosis and $250,000 from Centocor, and is an inventor on two patents on the use of peripheral blood gene expression patterns in the diagnosis of MS and PTSD. None of these are related to the current paper. None of the other authors has a financial relationship with a commercial entity that has an interest in the subject of this manuscript.

Acknowledgments: Chris Burton provided assistance with mouse husbandry. Dr. Donna Beers-Stolz assisted with imaging. Dr. Nancy Sussman provided valuable advice regarding statistical analysis.

References

1. Pack RJ, Al-Ugaily LH, Morris G. The cells of the tracheobronchial epithelium of the mouse: a quantitative light and electron microscope study. *J Anat* 1981;132:71–84.
2. Ten Have-Opbroek AA. Lung development in the mouse embryo. *Exp Lung Res* 1991;17:111–130.
3. Boers JE, Ambergen AW, Thunnissen FBJM. Number and proliferation of clara cells in normal human airway epithelium. *Am J Respir Crit Care Med* 1999;159:1585–1591.
4. Singh G, Katyal SL. Clara Cell Proteins. *Ann N Y Acad Sci* 2000;923:43–58.
5. Rawlins EL, Ostrowski LE, Randell SH, Hogan BL. Lung development and repair: contribution of the ciliated lineage. *Proc Natl Acad Sci USA* 2007;104:410–417.
6. Toskala E, Smiley-Jewell SM, Wong VJ, King D, Plopper CG. Temporal and spatial distribution of ciliogenesis in the tracheobronchial airways of mice. *Am J Physiol Lung Cell Mol Physiol* 2005;289:L454–L459.
7. Ten Have-Opbroek AA, De Vries EC. Clara cell differentiation in the mouse: ultrastructural morphology and cytochemistry for surfactant protein A and Clara cell 10 kD protein. *Microsc Res Tech* 1993;26: 400–411.
8. Fanucchi MV, Murphy ME, Buckpitt AR, Philpot RM, Plopper CG. Pulmonary cytochrome P450 monooxygenase and Clara cell differentiation in mice. *Am J Respir Cell Mol Biol* 1997;17:302–314.
9. Besnard V, Wert SE, Kaestner KH, Whitsett JA. Stage-specific regulation of respiratory epithelial cell differentiation by Foxa1. *Am J Physiol Lung Cell Mol Physiol* 2005;289:L750–L759.
10. Massaro GD, Davis L, Massaro D. Postnatal development of the bronchiolar Clara cell in rats. *Am J Physiol* 1984;247:C197–C203.
11. Stripp BR, Maxson K, Mera R, Singh G. Plasticity of airway cell proliferation and gene expression after acute naphthalene injury. *Am J Physiol* 1995;269:L791–L799.
12. Reynolds SD, Reynolds PR, Pryhuber GS, Finder JD, Stripp BR. Secretoglobins SCGB3A1 and SCGB3A2 define secretory cell subsets in mouse and human airways. *Am J Respir Crit Care Med* 2002;166: 1498–1509.
13. Homer RJ, Zhu Z, Cohn L, Lee CG, White WI, Chen S, Elias JA. Differential expression of chitinases identify subsets of murine airway epithelial cells in allergic inflammation. *Am J Physiol Lung Cell Mol Physiol* 2006;291:L502–L511.
14. Evans CM, Williams OW, Tuvim MJ, Nigam R, Mixides GP, Blackburn MR, DeMayo FJ, Burns AR, Smith C, Reynolds SD, *et al.* Mucin is produced by Clara cells in the proximal airways of antigen-challenged mice. *Am J Respir Cell Mol Biol* 2004;31:382–394.
15. Barth PJ, Wolf M, Ramaswamy A. Distribution and number of Clara cells in the normal and disturbed development of the human fetal lung. *Pediatr Pathol* 1994;14:637–651.
16. Pilette C, Godding V, Kiss R, Delos M, Verbeken E, Decaestecker C, De Paepe K, Vaerman JP, Decramer M, Sibille Y. Reduced epithelial expression of secretory component in small airways correlates with airflow obstruction in chronic obstructive pulmonary disease. *Am J Respir Crit Care Med* 2001;163:185–194.
17. Reynolds SD, Hong KU, Giangreco A, Mango GW, Guron C, Morinoto Y, Stripp BR. Conditional clara cell ablation reveals a self-renewing progenitor function of pulmonary neuroendocrine cells. *Am J Physiol Lung Cell Mol Physiol* 2000;278:L1256–L1263.
18. Reynolds SD, Giangreco A, Power JH, Stripp BR. Neuroepithelial bodies of pulmonary airways serve as a reservoir of progenitor cells capable of epithelial regeneration. *Am J Pathol* 2000;156:269–278.
19. Chomczynski P, Sacchi N. Single-step method of RNA isolation by acid guanidinium thiocyanate-phenol-chloroform extraction. *Anal Biochem* 1987;162:156–159.
20. Dolinay T, Kaminski N, Felgendreher M, Kim HP, Reynolds P, Watkins SC, Karp D, Uhlig S, Choi AM. Gene expression profiling of target genes in ventilator-induced lung injury. *Physiol Genomics* 2006;26:68–75.
21. Kaminski N, Friedman N. Practical approaches to analyzing results of microarray experiments. *Am J Respir Cell Mol Biol* 2002;27:125–132.
22. Selman M, Pardo A, Barrera L, Estrada A, Waston SR, Wilson K, Aziz N, Kaminski N, Zlotnik A. Gene expression profiles distinguish idiopathic pulmonary fibrosis from hypersensitivity pneumonitis. *Am J Respir Crit Care Med* 2006;173:188–198.
23. Reynolds SD, Shen H, Reynolds PR, Betsuyaku T, Pilewski JM, Gambelli F, Di Giuseppe M, Ortiz LA, Stripp BR. Molecular and functional properties of lung SP cells. *Am J Physiol Lung Cell Mol Physiol* 2007;292:L972–L983.
24. Heid CA, Stevens J, Livak KJ, Williams PM. Real time quantitative PCR. *Genome Res* 1996;6:986–994.

25. Reynolds SD, Giangreco A, Hong KU, McGrath KE, Ortiz LA, Stripp BR. Airway injury in lung disease pathophysiology: selective depletion of airway stem and progenitor cell pools potentiates lung inflammation and alveolar dysfunction. *Am J Physiol Lung Cell Mol Physiol* 2004;287:L1256–L1265.
26. Chichester CH, Philpot RM, Weir AJ, Buckpitt AR, Plopper CG. Characterization of the cytochrome P-450 monooxygenase system in nonciliated bronchiolar epithelial (Clara) cells isolated from mouse lung. *Am J Respir Cell Mol Biol* 1991;4:179–186.
27. Rodrigo L, Hernández AF, López-Caballero JJ, Gil F, Pla A. Immunohistochemical evidence for the expression and induction of paraoxonase in rat liver, kidney, lung and brain tissue: implications for its physiological role. *Chem Biol Interact* 2001;137:123–137.
28. Janmohamed A, Hernandez D, Phillips IR, Shephard EA. Cell-, tissue-, sex- and developmental stage-specific expression of mouse flavin-containing monooxygenases (Fmos). *Biochem Pharmacol* 2004; 68:73.
29. Terao M, Kurosaki M, Saltini G, Demontis S, Marini M, Salmona M, Garattini E. Cloning of the cDNAs coding for two novel molybdoflavoproteins showing high similarity with aldehyde oxidase and xanthine oxidoreductase. *J Biol Chem* 2000;275:30690–30700.
30. West JA, West JA, Williams KJ, Toskala E, Nishio SJ, Fleschner CA, Forman HJ, Buckpitt AR, Plopper CG. Induction of tolerance to naphthalene in Clara cells is dependent on a stable phenotypic adaptation favoring maintenance of the glutathione pool. *Am J Pathol* 2002;160:1115–1127.
31. Van Itallie CM, Rogan S, Yu A, Vidal LS, Holmes J, Anderson JM. Two splice variants of claudin-10 in the kidney create paracellular pores with different ion selectivities. *Am J Physiol Renal Physiol* 2006;291: F1288–F1299.
32. Coyne CB, Gambling TM, Boucher RC, Carson JL, Johnson LG. Role of claudin interactions in airway tight junctional permeability. *Am J Physiol Lung Cell Mol Physiol* 2003;285:L1166–L1178.
33. Inai T, Sengoku A, Guan X, Hirose E, Iida H, Shibata Y. Heterogeneity in expression and subcellular localization of tight junction proteins, claudin-10 and -15, examined by RT-PCR and immunofluorescence microscopy. *Arch Histol Cytol* 2005;68:349–360.
34. Weston WM, LeClair EE, Trzyna W, McHugh KM, Nugent P, Lafferty CM, Ma L, Tuan RS, Greene RM. Differential display identification of plunc, a novel gene expressed in embryonic palate, nasal epithelium, and adult lung. *J Biol Chem* 1999;274:13698–13703.
35. Giangreco A, Reynolds SD, Stripp BR. Terminal bronchioles harbor a unique airway stem cell population that localizes to the bronchoalveolar duct junction. *Am J Pathol* 2002;161:173–182.
36. Hong KU, Reynolds SD, Giangreco A, Hurley CM, Stripp BR. Clara cell secretory protein-expressing cells of the airway neuroepithelial body microenvironment include a label-retaining subset and are critical for epithelial renewal after progenitor cell depletion. *Am J Respir Cell Mol Biol* 2001;24:671–681.
37. Kim CF, Jackson EL, Woolfenden AE, Lawrence S, Babar I, Vogel S, Crowley D, Bronson RT, Jacks T. Identification of bronchioalveolar stem cells in normal lung and lung cancer. *Cell* 2005;121:823–835.